Instituto Nacional de Investigación y Tecnología Agraria y Alimentaria (INIA)
http://dx.doi.org/10.5424/sjar/2014122-4956

Spanish Journal of Agricultural Research 2014 12(2): 338-352
ISSN: 1695-971-X
eISSN: 2171-9292

RESEARCH ARTICLE

OPEN ACCESS

Microclimate evaluation of a new design of insect-proof screens in a Mediterranean greenhouse

Alejandro Lopez-Martinez, Diego L. Valera-Martinez*, Francisco Molina-Aiz, Araceli Peña-Fernandez and Patricia Marin-Membrive

Centro de Investigación en Biotecnología Alimentaria BITAL. Universidad de Almería. Ctra. de Sacramento, s/n. 04120 Almería, Spain

Abstract

This work studies natural ventilation in a Mediterranean greenhouse, comparing a new experimental screen of 13 × 30 threads cm^{-2} (porosity 39.0%) with a commercial control screen of 10 × 20 threads cm^{-2} (porosity 33.5%). In addition, both screens were tested in a wind tunnel to determine the discharge coefficients C_d of the greenhouse side and roof vents, which proved to be 0.16 for the commercial control screen and 0.18 for the experimental screen at both vents. These values represent a theoretical increase of 11% ($C_{d,\varphi\text{-}10\times20}/C_{d,\varphi\text{-}13\times30}=0.89$) in the natural ventilation capacity of the greenhouse when the experimental screen is used. The greenhouse was divided into two separate sections allowing us to analyze natural ventilation in both sectors simultaneously. Air velocity was measured in the lateral and roof vents with two 3D and six 2D sonic anemometers. Using the commercial control screen there was an average reduction of 16% in ventilation rate, and an average increase of 0.5°C in the average indoor air temperature, compared to the experimental screen. In addition, the ventilation efficiency η_T was higher with the experimental screen (mean value of 0.9) than with the control (mean value 0.6). We have designed an experimental insect-proof screen (13 × 30 threads cm^{-2}) with smaller thread diameter, higher thread density, smaller pore size and higher porosity than are used in most commercial meshes. All of these factors promote natural ventilation and improve the greenhouse microclimate.

Additional key words: natural ventilation; sonic anemometry; discharge coefficient; ventilation efficiency.

Introduction

With a view to reducing the entrance of certain insects in the greenhouse (aphids, leaf miners, whitefly, thrips or mealybugs), insect-proof screens are installed on the vents, thus reducing the need for phytosanitary treatments (Baker & Jones, 1989; Berlinger *et al*., 1992), while at the same time avoiding the exit of beneficial insects (Taylor *et al*., 2001; Teitel, 2007). On the other hand, the use of these materials reduces the greenhouses' capacity for natural ventilation (Muñoz *et al*., 1999; Fatnassi *et al*., 2003; Kittas *et al*.,

* Corresponding author: dvalera@ual.es
Received: 05-09-13 Accepted: 07-05-14.

Abbreviations used. **Nomenclature:** C_d (total discharge coefficient of the opening); $C_{d,LH}$ (discharge coefficient due to the shape of the opening); $C_{d,\varphi}$ (discharge coefficient due to the presence of insect-proof screens); D_f [thread density according to the manufacturer (threads cm^{-2})]; D_h [diameter of the threads (μm)]; D_i [diameter of the inside circumference of the pore (μm)]; D_r [thread density measurement (threads cm^{-2})]; E [thickness of the screen (μm)]; E_G [error in the calculation of volumetric flow rate (%)]; F_φ (pressure drop coefficient due to the presence of an insect-proof screen); G [mean volumetric flow rate (m^3 s^{-1})]; HR [relative air humidity (%)]; K_p [screen permeability (m^2)]; L_{px} [length of the pore in the weft direction (μm)]; L_{py} [length of the pore in the warp direction (μm)]; L_V [length of the vent (m)]; P [pressure (Pa)]; q [specific humidity (g g^{-1})]; R [ventilation rate (h^{-1})]; Re_p (Reynolds number based on the screen's permeability); R_o [incoming shortwave radiation (W m^{-2})]; S_A [greenhouse surface area (m^2)]; S_j [unit surface area corresponding to each measurement point in the vent (m^2)]; S_p [area of the pore (mm^2)]; S_V [vent surface area (m^2)]; T [temperature (°C)]; u [air velocity (m s^{-1})]; Y (inertial factor). **Greek letters:** Δ (difference); β [angle of opening (°)]; η_T (ventilation efficiency for the temperature); θ [wind direction (°)]; μ [dynamic viscosity of air (kg s^{-1} m^{-1})]; ρ_a [air density (kg m^{-3})]; φ [insect-proof screen porosity (%)]. **Subscripts:** *C* (corrected); *i* (inside); *j* (measurement point); *LS* (leeward side vent); *M* (average value); *O* (outside); *S* (sonic); *WR* (windward roof vent); *WS* (windward side vent); *x* (longitudinal component). **Superscripts:** * (corrected with wind speed); *c* (corrected with inside-outside air temperature).

2008; Baeza *et al*., 2009; Molina-Aiz *et al*., 2009), which has negative repercussions on the greenhouse microclimate, increasing the interior temperature and humidity (Fatnassi *et al*., 2006; Harmanto *et al*., 2006).

Growers must install insect-proof screens with an average pore size smaller than the size of the tiniest insect pest (Teitel, 2007), but at the same time the porosity of the chosen screens must not be detrimental to the natural ventilation of the greenhouse. Given this scenario, the growers' choice of mesh is limited, as lower porosity meshes reduce the ventilation rate and increase both temperature and humidity inside the greenhouse (Fatnassi *et al*., 2003). For instance, a mesh of 25% porosity can cause a drop in the greenhouse ventilation rate of 77-87% (Baeza *et al*., 2009); one of 53% porosity was found to reduce the ventilation rate by 50% and increase the greenhouse temperature by 4°C compared to a greenhouse without meshes (Bartzanas *et al*., 2002). Other studies have obtained the following results: 27% reduction in ventilation rate with a mesh of 50% porosity (Katsoulas *et al*., 2006), 50% reduction with a mesh of 45% porosity (Muñoz *et al*., 1999), 35% reduction with a mesh of 39% porosity (Pérez-Parra *et al*., 2004), 35% reduction with a mesh of 34% porosity (Campen & Bot, 2003), 38% reduction with a mesh of 34% porosity, and 55% reduction with a mesh of 26% porosity (Campen, 2005).

The above-mentioned negative aspects of the screens may be exacerbated by the accumulation of dust and dirt in the pores of the mesh (Linker *et al*., 2002; López *et al*., 2013). Over time the structure of the mesh deteriorates, and López *et al*. (2013) observed that the thread diameter increases by an average of 3.1% and the porosity of the screen suffers a mean reduction of 6.5%. The accumulation of dust and dirt in the insect-proof screens gives rise to a mean reduction in the porosity of the insect-proof screens of 20.3%. The combined total of these two negative effects (mesh degradation and accumulation of dust) amounted to a 26.8% mean reduction in porosity (López *et al*., 2013).

To avoid the entrance of insects into greenhouse, insect-proof screens are indispensable, but solutions must be sought to minimize their effect on the natural ventilation and the greenhouse microclimate. At this point several possibilities may be put forward:

— (i) Increasing the total ventilation surface in order to limit as much as possible the reduction in natural ventilation capacity brought about by the use of insect-proof screens (Muñoz *et al*., 1999; Teitel, 2007). One option is to increase the maximum angle to which the roof vent can be opened in multi-span greenhouses (Bailey, 2003), though this is hardly viable in areas with frequent strong winds. Another way is to fit the frames of the openings with pre-formed concertina-shape screens that unfold as the vents open and fold up again when they close (Bailey, 2003).

— (ii) Combining insect-proof screens with other means of pest control which allow the use of mesh with lower thread density and greater pore size. For instance, biological control methods making use of other insects, mites, fungi, bacteria, viruses, nematodes and weeds (auxiliary), which act as parasites, predators, pathogens, antagonists or competitors of the organisms that cause damage to the crop. The green revolution that Almería (Spain) has undergone over the last four years is particularly noteworthy. In this area many of the crops are produced using 100% biological control methods, which also constitute a competitive advantage over rival areas of production. The following examples provide an idea of the solutions available to growers: for the biological control of whitefly (*Trialeurodes vaporariorum* Westwood), the parasitic wasp *Encarsia formosa* (Castañé *et al*., 2004) can be used, and also autochthonous Mediterranean predatory bugs such as *Macrolophus caliginosus* or *Dicyphus tamaninii* Wagner (Lucas & Alomar, 2002; Castañé *et al*., 2004); to combat the *Bemisia argentifolii* whitefly parasitic wasps such as *Eretmocerus eremicus* and *Encarsia Formosa* (Hoddle *et al*., 1998) can be used; while to combat thrips (*Frankliniella occidentalis*), the parasitic nematode *Thripinema nicklewoodi* Siddiqi (Arthurs *et al*., 2003), the fungus *Metarhizium anisopliae* (Ansari *et al*., 2007), the predatory mite *Amblyseius cucumeris* or the wasp *Orius insidiosus* (Shipp & Wang, 2003) can all be used. Other methods for combating whitefly have been studied: planting a layer of covering vegetation that attracts these insects in order to reduce their incidence on crops (Hilje & Stansly, 2008); placing chromatographic adhesive traps shaped like a chrysanthemum flower (Mainali & Lim, 2008); and fitting electrostatic meshes (Tanaka *et al*., 2008).

— (iii) Designing new, more porous insect-proof screens with larger pores than the current marketed models. Along these lines, the present work presents an experimental mesh of 13×30 threads cm^{-2}. The threads of this mesh are of very small diameter, allowing us to obtain reduced pore size while at the same

time maintaining an acceptable level of porosity. This experimental insect-proof screen was designed by the "Rural Engineering" Research Group (AGR-198) of Almería University in collaboration with Spanish companies that manufacture and market such screens. The design allows the cost, and therefore the sale price, to be similar to that of screens currently on the market. The efficiency of the screen in preventing the entrance of whitefly into the greenhouse was tested using yellow sticky traps to calculate the whitefly population inside the experimental greenhouse described below over four crop cycles of *Solanum lycopersicum* L. In the first crop cycle (autumn-winter 2007/2008) a 66% reduction in whitefly population was observed in the western sector of the greenhouse fitted with the experimental mesh (13 × 30 threads cm^{-2}), as compared to the control mesh (10 × 20 threads cm^{-2}); in the second cycle (spring-summer 2008) this reduction was 12%; in the third one (autumn-winter 2008/2009) it was 7%; and in the fourth (spring-summer 2009) the reduction was 22% (Escamirosa, 2009).

Sonic anemometry has been used to study the effect of two insect-proof screens on the natural ventilation of a Mediterranean greenhouse; a commercial mesh (10 × 20 threads cm^{-2}) and the experimental one (13 × 30 threads cm^{-2}).

Material and methods

Two types of experiment have been carried out in order to evaluate the new design of insect-proof screens (13 × 30 threads cm^{-2}): A), wind tunnel tests to evaluate the aerodynamic characteristics of the experimental mesh (13 × 30 threads cm^{-2}) and the control mesh (10 × 20 threads cm^{-2}) in the laboratory (under controlled conditions); B), experimental measurements in the greenhouse, using two 3D and six 2D sonic anemometers, as well as other sensors, to analyze the microclimate and natural ventilation of the experimental greenhouse fitted with both screens.

Wind tunnel tests

In order to obtain the aerodynamic characteristics of the insect-proof screens, tests were carried out in a 4.74 m-long low velocity wind tunnel (Fig. 1) with a circular cross-section of 38.8 cm diameter. This wind tunnel was designed in the Engineering Department of the University of Almería. This device is able to produce airflows of up to 10 m s^{-1}, and is divided into the following principal parts (Fig. 1): flow conditioner and contraction, test section, diffuser and fan (Valera *et al*., 2006; Molina-Aiz *et al*., 2006). The experimental device forces a current of air through the porous meshes, allowing measurement of both the air velocity and the pressure drop produced. For the technical characteristics of the wind tunnel, the sensors used to measure air velocity and pressure drop and the different electronic components, see Valera *et al*. (2005 and 2006) or Molina-Aiz *et al*. (2006).

For geometric characterization of the insect-proof screens (Table 1) a specific software tool was used (Valera *et al*., 2003, 2006; Álvarez *et al*., 2012). The average diameter of the threads in the experimental screen (165.5 ± 7.0 µm) was much lower than that of the control screen (254.3 ± 11.7 µm) analysed by Álvarez (2010), and so its porosity was greater despite the higher density of threads.

Once we have determined the relationship between the pressure drop produced when the airflow passes through the mesh, the air velocity through the porous medium and the geometric characteristics of the meshes (porosity and thickness), we can calculate the screen permeability K_p, the inertial factor Y, the pressure drop coefficient F_φ and the discharge coefficient due to the presence of insect-proof screens $C_{d,\varphi}$.

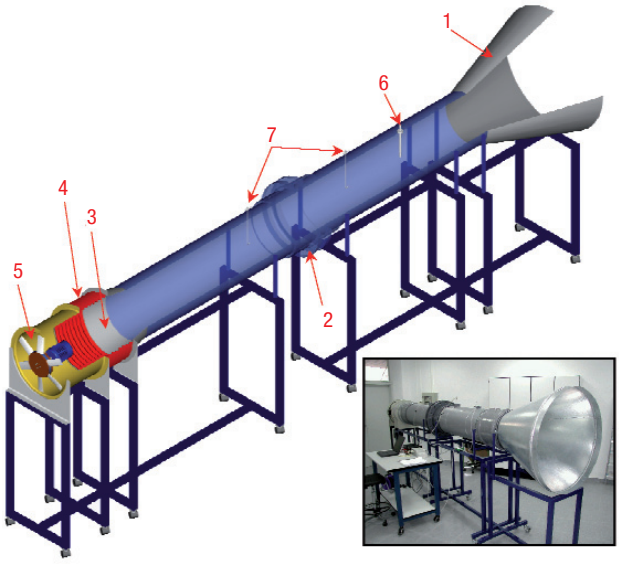

Figure 1. Low velocity wind tunnel designed at the University of Almería: (1) flow conditioner and contraction; (2) test section; (3) diffuser; (4) elastic joint clamp; (5) fan; (6) hot-film anemometer and temperature probe; (7) Pitot tubes.

Table 1. Geometric characteristics of the screens (average values ± standard deviation). D_f and D_r are the thread densities according to the manufacturer and measurement, respectively (threads cm^{-2}). Average value and standard deviation of: φ, porosity (m^2 m^{-2}); L_{px} and L_{py}, the lengths of the pore (μm) in the direction of the weft and warp, respectively; D_h, diameter of the threads (μm); D_i, diameter of the inside circumference of the pore (μm); S_p, area of the pore (mm^2)

	D_f	D_r	φ	L_{px}	L_{py}	D_h	D_i	S_p
Eastern sector	10 × 20	9.9 × 19.7	0.335 ± 0.011	233.7 ± 23.9	734.0 ± 29.2	274.5 ± 11.0	236.6 ± 24.0	0.171 ± 0.019
Western sector	13 × 30	13.1 × 30.5	0.390 ± 0.006	164.6 ± 9.3	593.3 ± 19.0	165.5 ± 7.0	167.4 ± 9.6	0.098 ± 0.006

Darcy's equation depends linearly on velocity for Reynolds numbers below the unit. However, for Reynolds number Re > 10 a break is observed in linearity, since the resistance to solid objects (in this case the mesh) is comparable to the resistance to friction with solid surfaces (Nield & Bejan, 1998). The airflow through the porous medium (the insect-proof screen) can be described by modifying Darcy's equation (Forchheimer, 1901):

$$\frac{\partial P}{\partial x} = -\left(\frac{\mu}{K_p} u + \rho_a \left(\frac{Y}{K_p^{1/2}} \right) |u| u \right) \quad [1]$$

where P is the pressure (Pa), x the direction of airflow, u the air velocity (m s^{-1}), Y the inertia factor, a dimensionless drag constant that depends on the characteristics of the porous material, K_p (m^2) is an independent coefficient of the nature of the fluid that depends on the geometry of the porous medium and is known as the specific permeability of the porous medium (Nield & Bejan, 1998), μ is the dynamic viscosity of air (kg s^{-1} m^{-1}) and ρ_a is the air density (kg m^{-3}). In line with Forchheimer's equation, a second degree polynomial can be used (Miguel *et al*., 1997; Dierickx, 1998; Muñoz *et al*., 1999) to adjust the experimental values of pressure drop through the mesh (Molina-Aiz *et al*., 2006; Valera *et al*., 2006):

$$\Delta P = au^2 + bu + c \quad [2]$$

The independent term cannot be considered if it is compared with the other terms (Miguel *et al*., 1997). Equating the coefficients of the first and second order terms of Forchheimer's Eq. [1] and of the second degree polynomial that results from the fit of the experimental data Eq. [2], we can obtain the specific permeability K_p (m^2) and the inertial factor Y (dimensionless) from the following expressions (Molina-Aiz *et al*., 2009):

$$K_p = e \frac{\mu}{b} \quad [3]$$

$$Y = \frac{a K_p^{0.5}}{\rho_a e} \quad [4]$$

where e is the thickness of the screen (m). To obtain an accurate measurement of the thickness of the mesh, dimensional contact-free metrology has been used. The optical measurements were taken with a TESA-VISIO 300 (TESA SA, Switzerland) fitted with video and with a resolution of 0.05 μm and an uncertainty in measurement of (3 + 10 · e/1,000) (μm), where e is the dimension measured, in this case the thickness of the mesh. For the magnitude of the measurements taken the uncertainty was less than 10 μm.

Bernoulli's equation can also be used to describe the relationship between pressure drop and air velocity through the mesh (Kosmos *et al*., 1993; Montero *et al*., 1997; Teitel & Shklyar, 1998):

$$\Delta P = -\frac{1}{2} F_\varphi \rho_a u^2 \quad [5]$$

where F_φ is the pressure drop coefficient due to the presence of an insect-proof screen. This coefficient can be calculated from the wind tunnel tests according to the expression obtained by equaling Eq. [1] and Eq. [5] for $\partial P/\partial x = \Delta P/e$ (Molina-Aiz *et al*., 2009):

$$F_\varphi = \frac{2e}{K_p^{0.5}} \left(\frac{1}{\mathrm{Re}_p} + Y \right) \quad [6]$$

This coefficient can be used to predict the pressure drop through the mesh for Reynolds numbers $\mathrm{Re}_p < 10^5$ (Teitel, 2001). Re_p is the Reynolds number based on the screen's permeability and it can be calculated by considering the square root of specific permeability K_p (Nield & Bejan, 1998):

$$\mathrm{Re}_p = \frac{\sqrt{K_p} u \rho_a}{\mu} \quad [7]$$

In the present study, to determine Re_p we have used a value of 0.25 m s^{-1} for u (maximum mean value of the longitudinal component u_x, perpendicular to the vents, in the experimental greenhouse). The discharge coefficient due to the presence of insect-proof screens $C_{d,\varphi}$ can be calculated from the pressure drop coefficient F_φ as follows (Molina-Aiz *et al*., 2009):

$$C_{d,\varphi} = 1 / F_{\varphi}^{0.5} \quad [8]$$

Bernouilli's law establishes that when a vent is opened the pressure drop between its two sides (potential energy) becomes kinetic energy. The main parameters that determine the aerodynamic behavior of the vents are their geometry (height and width), the angle to which they are opened and the presence of insect proof screens (porosity and airflow). The coefficient C_d for each vent can be calculated as follows (Arbel *et al*., 2000; Kittas *et al*., 2002; Teitel, 2007):

$$C_d = \sqrt{\frac{1}{\frac{1}{C_{d,LH}^2} + \frac{1}{C_{d,\varphi}^2}}} \quad [9]$$

where $C_{d,LH}$ is the discharge coefficient due to the shape of the opening which can be obtained as follows (Bailey *et al*., 2003):

$$C_{d,LH} = \left\{1.9 + 0.7\exp\left[-L_V / \left(32.5 h \sin\beta\right)\right]\right\}^{-0.5} \quad [10]$$

where L_V is the length of the vent [m], h the height (m) and , the angle of opening, which is 90° for side vents without spoiler and 14° for the roof vent.

Experimental setup for greenhouse measurements

The experimental measurements were carried out in a multi-tunnel greenhouse (24 × 45 m^2), divided into two sectors (eastern sector 24 × 25 m^2 and western sector 24 × 20 m^2), located at the "Catedrático Eduardo Fernández" farm of the UAL-ANECOOP Foundation (36° 51' N, 2° 16' W) in the province of Almería (Fig. 2). The greenhouse was divided in two parts by a three-layer plastic film of the same material as the greenhouse cover. The plastic was held in place using metal profiles which are the same as those used on the greenhouse side walls, and in this way no air could pass from one sector to the other. Experimental measurements were carried out during the spring-summer crop cycle of *Solanum lycopersicum* L. cv. Salomee (average height 1.20 and 1.88 m, and average leaf area index (LAI) 0.78 and 2.75 m^2 m^{-2}, for the first and the last experimental measurements, respectively).

One roof vent and both side vents were fully open during the experimental measurements (Fig. 2, Table 2). The commercial insect-proof screen control (10 × 20 threads cm^{-2}; Fig. 3a) was placed on the vents in the eastern sector of the greenhouse, while the experimental one (13 × 30 threads cm^{-2}; Fig. 3b) with a higher thread density was installed in the western sector.

Table 2. Dimensions of the vents [m^2]. S_V/S_A, ratio of vent surface/greenhouse surface [%]

	Northern side vent	Southern side vent	Roof vent	S_V/S_A
Eastern sector	1.05 × 22.5	1.05 × 22.5	1.00 × 22.5	11.6
Western sector	1.05 × 17.5	1.05 × 17.5	1.00 × 17.5	11.3

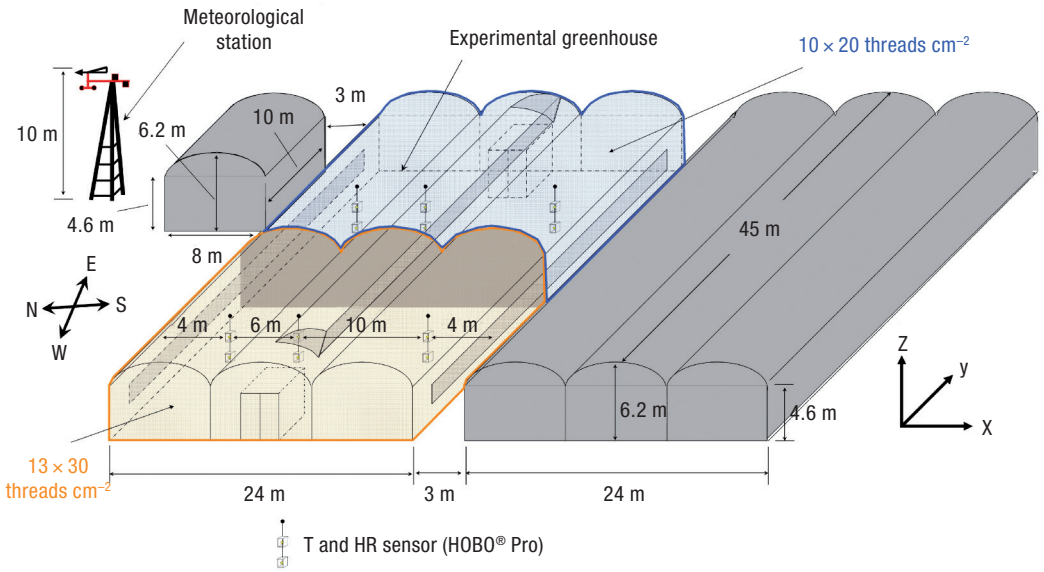

Figure 2. Location of the experimental greenhouse at the farm.

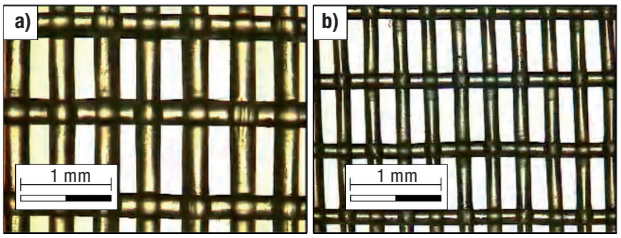

Figure 3. Microscope image of the control mesh 10 × 20 threads cm^{-2} (a) and the experimental mesh 13 × 30 threads cm^{-2} (b).

The natural ventilation of the greenhouse was studied in both sectors simultaneously. The air velocity was measured at 12 points in each side vent (Fig. 4a) and at 3 points in each roof vent (Fig. 4b). The vent area corresponding to each measurement point was 2.0 m^2 (side vents) and 7.5 m^2 (roof vent) in the eastern sector, and 1.5 m^2 (side vents) and 5.8 m^2 (roof vent) in the western sector. These values are similar to those used by Boulard *et al*. (1998) in a tunnel greenhouse with one roof vent (2.6 m^2 per point), by Teitel *et al*. (2008) in a mono-span greenhouse with two side vent openings (1.1 m^2 per point), by Teitel *et al*. (2005) in a four-span greenhouse with three roof vents (8.5 m^2 per point) and by Molina-Aiz *et al*. (2009) in a five-span Almería-type greenhouse (2.1 m^2 per point).

Two 3D and six 2D sonic anemometers were used: half of the total in each sector. The 3D anemometers measured the air velocity over 3 minutes (Molina-Aiz *et al*., 2009; López *et al*., 2011, 2012) at each point in the side vents (Fig. 4c). The 2D anemometers were

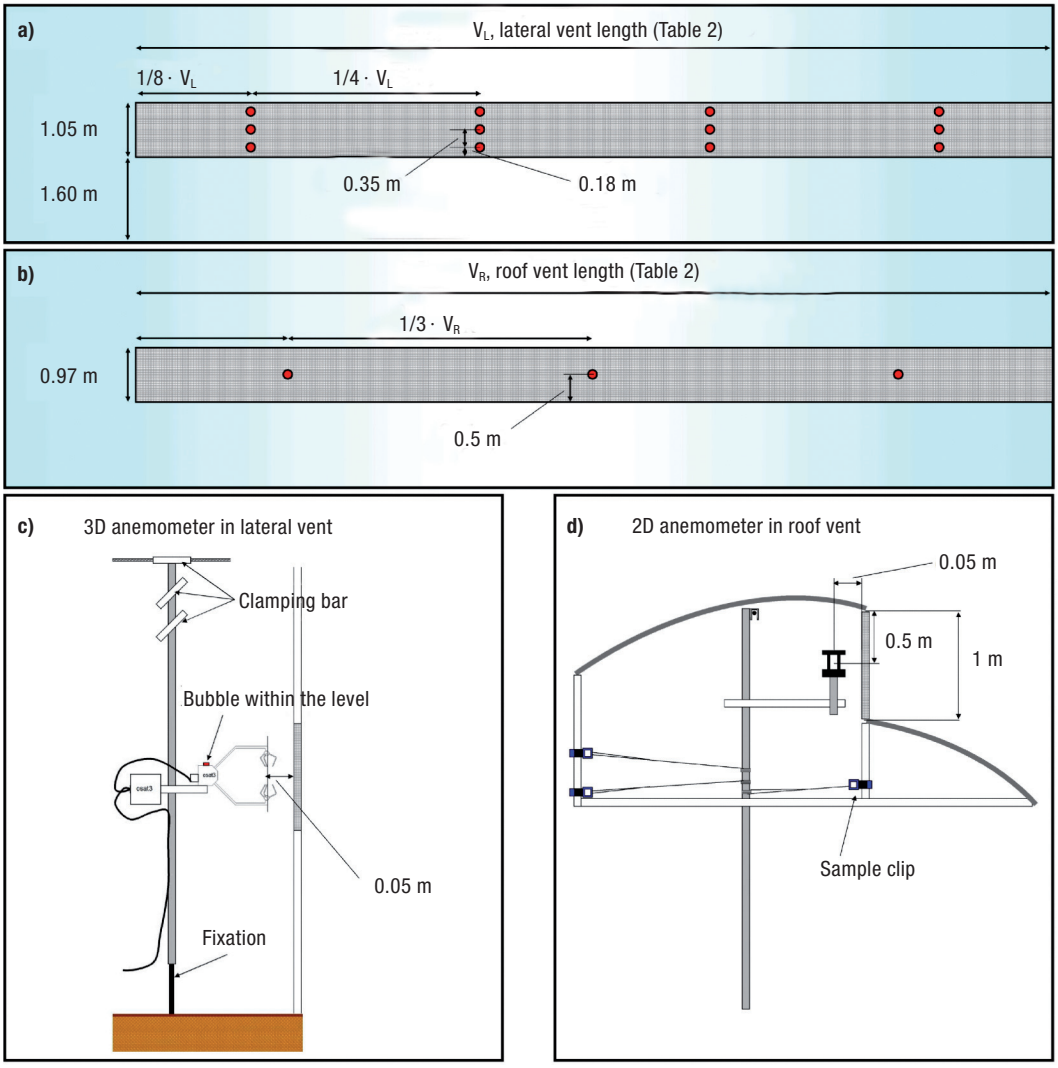

Figure 4. Measurement points at the side vents (a) and roof vents (b). Details of the experimental setup using 3D anemometers placed at the side vents (c) and 2D anemometers at the roof vent (d).

used to measure continuously the air velocity at each point in the roof vent (Fig. 4d). The methodology employed has been explained in greater detail in López *et al*. (2011, 2012).

The side vent of the northern sector of the greenhouse was partially blocked by a small auxiliary warehouse (Fig. 2). This implies a negative influence on the experimental design, as the two sectors of the greenhouse are not identical. In order to complement the results obtained from the experimental measurements (B), wind tunnel tests (A) were also carried out. In this way the aerodynamic behaviour of the mesh was analyzed without the influence of external factors.

Instrumentation

Air velocity and temperature were measured with two CSAT3 3D sonic anemometers (Campbell Scientific Spain S.L., Spain; resolution: 0.001 m s^{-1} and 0.002°C; accuracy ± 0.04 m s^{-1} and ± 0.026°C). The air velocity was also measured with 6 Windsonic 2D sonic anemometers (Gill Instrument LTD, Lymington, Hampshire, UK; resolution: 0.01 m s^{-1}; accuracy 2%). The data from all sonic anemometers were recorded by two CR3000 Microloggers (Campbell Scientific Spain S.L., Barcelona, Spain), with a data registration frequency of 10 Hz (Shilo *et al*., 2004) for the 3D and 1 Hz for the 2D sonic anemometers (López *et al*., 2011 and 2012).

Outside climatic conditions were recorded by a meteorological station at a height of 10 m (Fig. 2). The meteorological station included a BUTRON II (Hortimax S.L., Almería, Spain) measurement box with a Pt1000 temperature sensor and a capacitive humidity sensor, with a temperature measurement range of –25°C to 75°C and accuracy of ± 0.01°C, and a humidity range of 0% to 100% and accuracy of ± 3%. Outside wind speed was measured with a Meteostation II (Hortimax S.L.), incorporating a cup anemometer with a measurement range of 0 to 40 m s^{-1}, accuracy of ± 5%, and resolution of 0.01 m s^{-1}. Wind direction was measured with a vane (accuracy ± 5° and resolution 1°). Solar radiation was measured using a Kipp Solari (Hortimax S.L.) sensor, with a measurement range of 0 to 2,000 W m^{-2}, accuracy of ± 20 W m^{-2}, and resolution of 1 W m^{-2}.

Temperature and humidity inside the greenhouse were measured using 12 autonomous dataloggers (HOBO Pro Temp-HR U23-001, Onset Comput. Corp., Bourne, MA, USA) placed at heights of 1 and 2 m. These fixed devices allowed temperature measurement in a range of –40°C to 70°C with an accuracy of ± 0.18°C. They were all programmed to register data at 0.5 Hz and were protected against direct solar radiation with passive solar radiation open boxes, allowing natural air movement around the sensors (Molina-Aiz *et al*., 2004). From the data of inside humidity we can obtain the specific humidity q and correct the sonic anemometer temperature T_s using the following expression (Tanny *et al*., 2008):

$$T_{sc} = \frac{T_s}{1 + 0.51q} \quad [11]$$

Statistical analysis

Temperature data inside the different sectors of the experimental greenhouse were subjected to Analysis of Variance (ANOVA) using Statgraphics Plus 4.1 Software (Manugistics, Inc., Rockville, MD, USA). One-way ANOVA and possible significant differences between the temperature inside the eastern and western sectors were evaluated by Least Significant Differences (LSD) multiple comparison tests with a confidence level of 95%. On the other hand, regression analyses were carried out to study the relationship between the inside temperature (T_i), as dependent variable, and the outside temperature (T_o), the wind speed (u_o) and the porosity of the insect-proof screens (φ), as independent variables.

Calculation of the airflow passing through the vents

With only one sampling position possible (for lateral vents) at any one time, a difficulty arises from how to deal with changing external conditions throughout the time needed to record data at all the measurement positions in the lateral vents of each sector. This problem can be overcome by correcting the air velocities measured by the 3D sonic anemometer at each position j at the lateral vents through a process of scaling with the wind speed (Boulard *et al*., 2000; Molina-Aiz *et al*., 2009; López *et al*., 2011):

$$u^*_{x,j} = \frac{u_{x,j}}{u_{o,j}} u_o \quad [12]$$

where u_o is the mean wind speed during the experimental measurements [m s^{-1}], $u_{o,j}$ and $u_{x,j}$ the mean va-

lue of the wind speed and of the longitudinal component of the air velocity u_x corresponding to measurement point j. The volumetric flow rate G is calculated by multiplying $u^*_{x,j}$ by the vent surface area corresponding to each measurement point (Boulard *et al*., 1998):

$$G = \sum_{j=1}^{m} S_j u^*_{x,j} \qquad [13]$$

Results and discussion

Wind tunnel tests

The tests in the wind tunnel (Table 3) allowed the discharge coefficient $C_{d,\varphi}$ to be determined (for $u = 0.25$ m s^{-1}) as 0.17 for the control screen (10 × 20 threads cm^{-2}) and as 0.19 for the experimental one (13 × 30 threads cm^{-2}). The discharge coefficient C_d for the side and roof vents was then calculated as 0.16 for the control and 0.18 for the experimental screen at both vents. These values are similar to those obtained in other studies on insect-proof screens: $C_d = 0.253$ in a mono-span greenhouse with side vents and a mesh of 35% porosity (Teitel *et al*., 2008); $C_d = 0.194$ for an Almería-type greenhouse with a mesh of 34% porosity (Molina-Aiz *et al*., 2009). In the latter, the authors report the values obtained in a number of other works, ranging between 0.42 and 0.89 for vents without screens and between 0.16 and 0.51 for vents with insect-proof screens of 25% and 45% porosity, respectively.

Fatnassi *et al*. (2002) establish that the relationship between the ventilation rates of the same greenhouse with and without insect-proof screens can be considered as proportional to the ratio of the discharge coefficients of the vents with and without screens. Bearing this in mind, the results obtained would lead us to expect a theoretical increase of 11% ($C_{d\text{-}10\times20}/C_{d\text{-}13\times30} = 0.89$) in the natural ventilation capacity in the greenhouse's western sector fitted with the experimental screen (13 × 30 threads cm^{-2}) with respect to that of the eastern sector with the commercial screen (10 × 20 threads cm^{-2}). The vents' discharge coefficients were also calculated for values of u from 0.05 to 0.50 m s^{-1} (Fig. 5), and in all cases the $C_{d\text{-}10\times20}/C_{d\text{-}13\times30}$ ratios obtained were equal to 0.89.

Table 3. Aerodynamic characteristics of the insect-proof screens: e, thickness (μm); a, b and c are the coefficients of the polynomial fit from the wind tunnel tests (Eq. [5]); R^2, the fit determination coefficient; K_p, screen permeability (m^2); Y, inertial factor; F_φ, pressure drop coefficient due to the presence of an insect-proof screen; $C_{d,\varphi}$, discharge coefficient due to the presence of insect-proof screens (for $u = 0.25$ m s^{-1}); $C_{d,LH}$, discharge coefficient due to the shape of the opening; C_d, total discharge coefficient of the opening; Re, Reynolds number

Screen	10 × 20	13 × 30
e	563.8	391.7
a	2.495	1.683
b	4.797	3.731
c	–1.248	0.344
R^2	0.999	0.999
K_p	$2.12 \cdot 10^{-9}$	$1.93 \cdot 10^{-9}$
Y	0.169	0.159
F_φ	$24.46 \cdot (0.169 + \mathrm{Re}^{-1})$	$17.84 \cdot (0.159 + \mathrm{Re}^{-1})$
$C_{d,\varphi}$	0.167	0.189
$C_{d,LH\text{-}Side}$	0.665	0.657
$C_{d,LH\text{-}Roof}$	0.719	0.712
$C_{d\text{-}Side}$	0.162	0.181
$C_{d\text{-}Roof}$	0.162	0.182

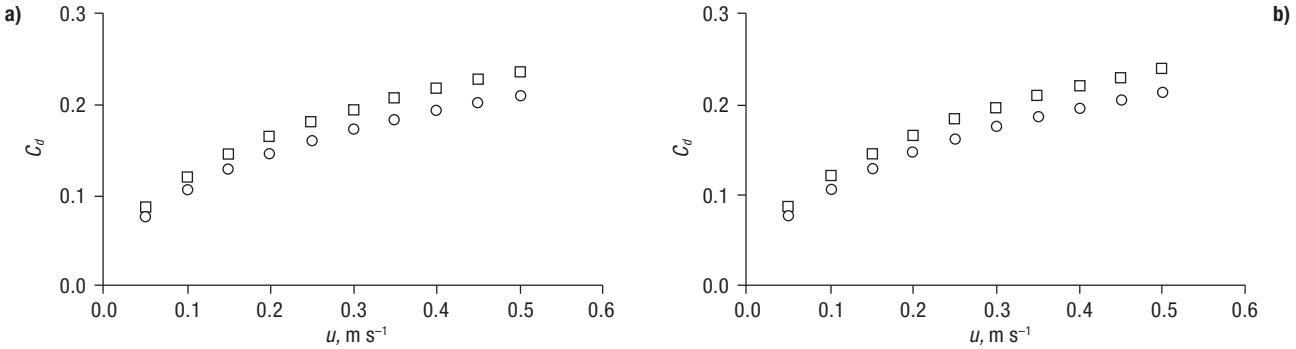

Figure 5. Discharge coefficient (C_d) at the side vent (a) and roof vent (b) as a function of air velocity (u). □, mesh 13 × 30 threads cm^{-2}; ○, mesh 10 × 20 threads cm^{-2}.

Experimental measurements in greenhouse

The measurement tests were carried out under *Poniente* wind from the southwest. The outside climatic conditions remained relatively stable over the six measurement tests (Table 4).

Airflow

Given the characteristics of the experimental greenhouse (with a windward facing roof vent, a windward facing side vent that is blocked by another greenhouse and a leeward facing side vent which is partially blocked in the eastern sector) the eolic and thermal effects are contrary. Due to the eolic effect the incoming air enters through the roof vent (wind pressure) and exits through the leeward side vent (suction of the wind), but also through the windward side vent, as it is in the shelter of the adjacent greenhouse. Due to the thermal effect, the hot air rises to exit through the roof vent, which favours the entrance of air from outside through the side vents. The combination of these two effects at the three vents means that there are opposing incoming and outgoing airflows (Fig. 6). The same ventilation pattern was previously observed for the western sector of the greenhouse under prevailing *Poniente* winds (López *et al*., 2011 and 2012).

Despite the difference in porosity of the tested screens (5.5 points), no major differences were found in the ventilation patterns of the two greenhouse sectors (Fig. 6).

The greenhouse ventilation is affected by the buoyancy effect generated by the average characteristic temperature difference between the inside and the outside air ΔT_{io}. Papadakis *et al*. (1996) showed that the effect of buoyancy on greenhouse ventilation could not be neglected at wind speeds lower than about 1.8 m s^{-1}. In greenhouses with both roof and side openings, Kittas *et al*. (1997) considered that the stack effect is important if the ratio $u_o/\Delta T_{io}^{0.5} < 1$. In the present case, air was found to both enter and leave the greenhouse through the roof vent in all experimental measurements, which indicates that the thermal effect played a major role in the natural ventilation, even though the ratio $u_o/\Delta T_{io}^{0.5}$ was at times higher than 1 (Table 4).

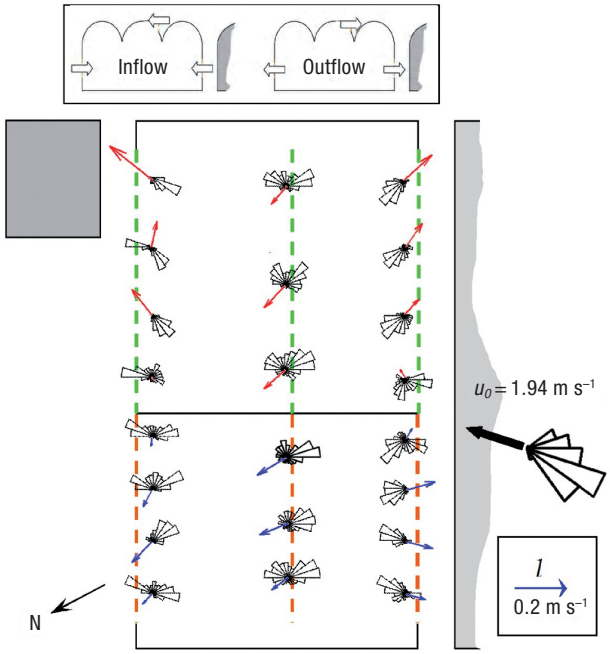

Figure 6. Airflow at the vents during experimental measurement number 1 (height of measurements at the side vents 2.13 m). Eastern sector with the control mesh 10 × 20 threads cm^{-2} (green mesh, red vectors) and western sector with the experimental mesh 13 × 30 threads cm^{-2} (orange mesh, blue vectors).

Table 4. Outside climatic conditions (average values ± standard deviation): u_o, outside wind velocity [m s^{-1}]; θ, wind direction [°]; HR_o, outside relative air humidity [%]; T_o, outside temperature [°C]; R_o, incoming shortwave radiation [W m^{-2}]; N, experimental measurement number

	N - Date	Time	u_o	θ^a	HR_o	T_o	R_o	$u_o/\Delta_{io}^{0.5}$ (10 × 20)	$u_o/\Delta_{io}^{0.5}$ (13 × 30)
1	17/04/2009	11:06-13:07	1.94 ± 0.70	226 ± 25	59 ± 5	16.9 ± 0.4	584 ± 175	0.65	0.65
2	23/04/2009	11:23-13:16	2.34 ± 0.98	267 ± 14	38 ± 2	22.1 ± 0.6	809 ± 56	0.92	0.94
3	22/06/2009	11:14-12:58	3.42 ± 0.50	258 ± 8	56 ± 4	25.5 ± 0.4	617 ± 71	2.08	2.55
4	26/06/2009	11:17-13:04	2.67 ± 0.72	227 ± 20	64 ± 2	24.0 ± 0.5	751 ± 102	1.23	1.29
5	02/07/2009a	11:00-12:45	2.62 ± 0.63	239 ± 17	65 ± 3	27.0 ± 0.9	725 ± 68	1.26	1.34
6	02/07/2009b	14:41-16:28	3.22 ± 0.48	242 ± 14	60 ± 2	28.0 ± 0.8	868 ± 37	1.47	1.57

[a] Direction perpendicular to the vents is 208° for a Poniente wind from southwest (SW).

Air exchange rate

The precision of the average air exchange measurements can be checked by summing inflows and outflows (Boulard *et al*., 1996) through all the openings' surfaces in order to verify the degree to which mass conservation in the greenhouse is satisfied (Boulard *et al.,* 1997). The mean ventilation flux G_M has been calculated from Eq. [13] using velocities scaled with the wind speed Eq. [12] and reducing the average difference between outflow and inflow to 11.8% and 67.0% for the western and eastern sectors, respectively (Table 5).

Surprisingly, although the same methodology was followed and the tests were carried out simultaneously, the average difference between outflow and inflow in the western sector was much less than that in the eastern one. This major difference may well be attributed to the partial blockage at the northern section of the side vent in the eastern sector (Fig. 2), which surely affects the airflow at that vent. More measurement points would therefore be required at that vent. In the western sector, on the other hand, where there are no obstacles, the airflow is more uniform at all vent surfaces, and therefore the number of measurement points is considered to be sufficient.

The air exchange rates observed in the present work (Table 5) are very low in both sectors when compared to recommended values, which for a temperature rise of 5°C between exit and inlet air temperatures vary from 0.02 $m^3\ s^{-1}\ m^{-2}$ to 0.09 $m^3\ s^{-1}\ m^{-2}$ (15 to 65 h^{-1} for a greenhouse with an average height of 5 m) depending on the solar radiation and the crop transpiration (ASABE Standards, 2008), with optimum values of between 45 and 60 h^{-1} (Hellickson & Walker, 1983). An air exchange rate of at least 45 h^{-1} would limit the inside-outside thermal gradient to approximately 5°C (Molina-Aiz, 2010). There are two main reasons for these low rates: (i) the combination of vents in the greenhouse gives rise to opposing wind and thermal effects; (ii) the insect-proof screens drastically reduce the discharge coefficients C_d at the vents as compared to the obtained values of the coefficient $C_{d,LH}$, which is an approximation of the values at vents without screens (Table 3). Below we indicate the values of air exchange rates observed by other authors using similar methodology, *i.e.* sonic anemometers in greenhouses with insect-proof screens: in an Almería-type greenhouse (S_A = 1,750 m^2; screen porosity = = 34%), with two side vents and two roof vents, Molina-Aiz *et al*. (2009) observed values for R_M from 5.0 to 16.8 h^{-1} (for u_o from 3.34 to 8.40 m s^{-1}, respectively); in a mono-span greenhouse (S_A = 74.4 m^2; screen porosity = 35%), with two side vents, Teitel *et al*. (2008) observed values for R_M of 20.7 h^{-1} (u_o = 4.5) and 15.7 h^{-1} (u_o = 4.6 m s^{-1}). The R_M values observed in the present work are similar to those found by Molina-Aiz *et al*. (2009) at similar wind speeds. The higher air exchange rate recorded by Teitel *et al*. (2008) is mainly

Table 5. Ventilation volumetric flow rates [$m^3\ s^{-1}$] through each vent opening calculated from Equation [3] with values of longitudinal component of air velocitiy u_x^* corrected with wind speed: leeward side G_{LS}, windward side G_{WS}, and windward roof G_{WR}. Error in the calculation of ventilation flow rates E_G [%] and air exchange rate R_M [h^{-1}]. N, experimental measurement number

N	Date	G_{LS}	G_{WS}	G_{WR}	G_M	$E_G = \frac{\Delta G}{G_M}$	R_M
10 × 20							
1	17/04/2009	0.16	–0.95	1.60	1.36	59.6	1.45
2	23/04/2009	0.46	–2.07	1.46	1.99	–7.4	2.13
3	22/06/2009	–0.35	–4.14	2.36	3.42	–62.2	3.66
4	26/06/2009	–0.36	–3.87	1.84	3.03	–78.7	3.24
5	02/07/2009	–0.55	–3.26	1.12	2.47	–109.1	2.64
6	02/07/2009	–1.54	–4.98	2.64	4.58	–84.8	4.90
13 × 30							
1	17/04/2009	–0.10	–1.46	1.59	1.57	1.8	2.11
2	23/04/2009	0.29	–1.98	1.94	2.11	12.3	2.83
3	22/06/2009	–1.50	–3.07	4.30	4.44	–6.3	5.96
4	26/06/2009	0.47	–2.64	2.03	2.57	–5.3	3.46
5	02/07/2009	–0.19	–2.02	1.80	2.01	–20.8	2.69
6	02/07/2009	–1.17	–2.57	2.93	3.33	–24.3	4.48

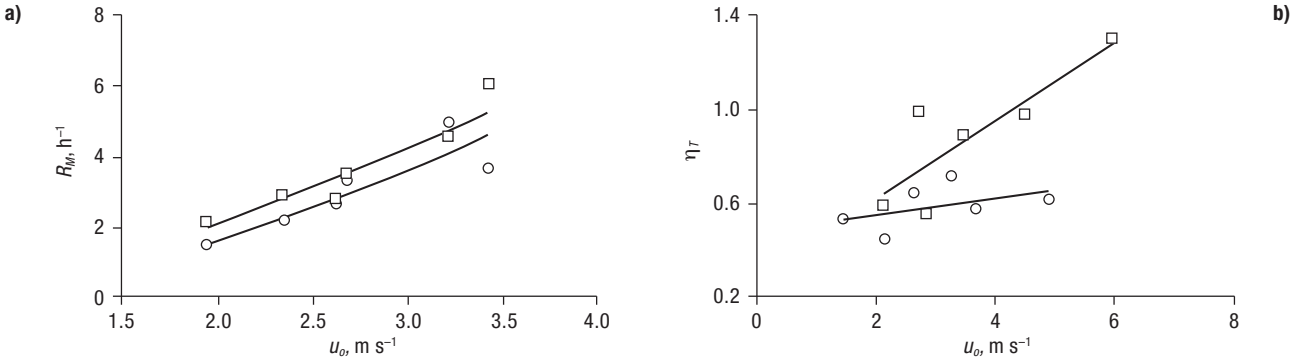

Figure 7. Air exchange rate R_M (a) and ventilation efficiency for the temperature η_T (b). □, western sector with the experimental mesh 13 × 30 threads cm^{-2}; ○, eastern sector with the control mesh 10 × 20 threads cm^{-2}.

due to the small dimensions of the greenhouse used, with a distance between vents of only 9.3 m and a greenhouse volume of approximately 300 m^3.

The lower porosity of the control screen (33.5% as opposed to 39% for the experimental one) may well be the main cause of the reduction in air exchange rate observed in the eastern sector (Table 5, Fig. 7a). However, the partial obstacle at the northern end of the eastern sector might also contribute to the reduction. Bearing in mind the exchange rate R_M calculated from the average flow G_M, a 16% mean reduction in R_M is found in the eastern sector (with a ratio $R_{M\text{-}10\times20}/R_{M\text{-}13\times30}$ = = 0.84). The maximum reduction in the air exchange rate, R_M = 39%, was recorded in test 3 (Table 5).

The results of the wind tunnel tests indicated that the different aerodynamic characteristics of the insect-proof screens lead to a theoretical 11% reduction in the ventilation capacity of the eastern sector compared to the western one ($C_{d\text{-}10\times20}/C_{d\text{-}13\times30}$ = 0.89). The difference between $C_{d\text{-}10\times20}/C_{d\text{-}13\times30}$ = 0.89 and $R_{M\text{-}10\times20}/R_{M\text{-}13\times30}$ = 0.84 is thought to be due in the main to the influence of the obstacle that partially blocks the eastern sector of the greenhouse. In addition, it is important to remember that the ventilation surface in the eastern sector (S_V/S_A = 11.6) is slightly larger than that in the western one (S_V/S_A = 11.3).

The difference in the ventilation rate observed for the two types of mesh tested (5% difference in porosity) differs considerably from the results of Harmanto *et al*. (2006), who observed that two different meshes (30% and 38% porosity) reduced the ventilation rate by 50% and 35%, respectively, when compared to a third mesh of 41% porosity. Fatnassi *et al*. (2003) found that a mesh of 19% porosity reduced the air velocity inside the greenhouse by 50% as compared to a mesh of 69% porosity. The differences between the results recorded by Harmanto *et al*. (2006) and Fatnassi *et al.* (2003) are due to the different experimental methods employed. Harmanto *et al*. (2006) worked with water vapor mass balance and energy balance methods; while Fatnassi *et al*. (2003) worked with simulations based on Computer Fluid Dynamics (CFD). The method followed and the placement of the sensors in each case can have a significant bearing on the results obtained. Van Buggenhout *et al*. (2009) studied the influence of the position of sensors on results when the tracer gas method is employed, and they found that the errors involved reached up to 86%. This fact should therefore be taken into account, especially when the tracer gas method is used to validate CFD simulations, as is the case of Fatnassi *et al*. (2003).

Interior microclimate

The greenhouse microclimate was monitored while the experimental measurements were being carried out (approx. 2 h). The 3D anemometers were used to determine the temperature at each of the measurement points in the side vents consecutively for 3 min each. The effect of changes in outside temperature throughout the duration of the tests should be considered. To do so, we have used the average inside and outside temperatures as the parameter to scale the inside temperature measured with the anemometers (López *et al*., 2012):

$$T^c_{sc,j} = T_{sc,j}\frac{\left(T_o + T_i\right)}{\left(T_{o,j} + T_{i,j}\right)} \qquad [14]$$

where $T_{sc,j}$ is the corrected sonic temperature (Eq. [11]) for position j in the lateral vents, T_o and T_i are the mean outside and inside air temperatures during the test and $T_{o,j}$ and $T_{i,j}$ are the mean outside and inside air

temperatures recorded by the fixed sensors over the 3 min used for measurement at position *j*.

In order to judge objectively the effect of ventilation on the inside temperature, we have determined the ventilation efficiency for the temperature η_T (Qingyan *et al*., 1988):

$$\eta_T = \frac{T_{i-o} - T_o}{\Delta T_{io}} \qquad [15]$$

where T_{i-o} is the mean temperature of the air that leaves the greenhouse through the side vents and ΔT_{io} is the difference in temperature between inside and outside the greenhouse during the course of the experimental measurements. The term η_T represents the effectiveness to eliminate heat of the greenhouse area occupied by the crop. A value of η_T equal to 1 indicates that the outside air enters into greenhouse and it mixes perfectly with the inside air.

A mean drop in the inside temperature of 0.5°C was observed in the sector with the experimental mesh, compared to the sector that was fitted with the commercial model (Table 6). The maximum temperature difference between both sectors (0.9°C) was recorded during experimental measurement number 3. The lower air exchange rate recorded in the sector with the commercial mesh means that there is less capacity of natural ventilation to force out the heat from the greenhouse. The ventilation efficiency was always greater in the sector which was fitted with the experimental mesh (mean value of $\eta_T = 0.9$) than in the one with the commercial mesh (mean value of $\eta_T = 0.6$) (Fig. 7b).

In the western sector with the experimental mesh, where there was no obstacle by the leeward facing side vent, the air that entered the greenhouse through the roof vent mixed better with the air in the crop zone and left the greenhouse through the side vents, at higher temperature than the air in the eastern sector with the control mesh.

The results obtained in the present work confirm the mean increase in temperature observed by Harmanto *et al*. (2006), *i.e.* 0.1°C for each percentage point difference in the porosity of the screens. The increase in the temperature difference ΔT_{io} due to the lower porosity of the control mesh, expressed as the ratio $\Delta T_{io\text{-}10 \times 20} / \Delta T_{io\text{-}13 \times 30} = 1.16$, is similar to the value of 1.25 recorded by Kittas *et al*. (2002), who compared meshes of de 50 and 60%. Fatnassi *et al.* (2003, 2006) obtained different values for the same ratio, 1.50, 1.43 and 2.67, recorded between meshes of 29 and 40%; of 20 and 41%, and of 56 and 69% porosity, respectively.

The statistical analysis based on the multiple regression between the porosity of the mesh φ (per 1%), the inside and outside temperatures T_i and T_o (°C) and the air velocity u_o (m s^{-1}) provide us with the following expression:

$$T_i = 0.8 \cdot T_o - 2.5 \cdot u_o - 9.4 \cdot \varphi + 20.4 \qquad [16]$$
$$\left(R^2 = 86.1\%;\ p\text{–}value = 0.001\right)$$

The inside temperature increases with the outside temperature and decreases with the air velocity and porosity. A 10% increase in the mesh porosity gives rise to a 0.9°C drop in inside temperature, while a 1 m s^{-1} increase in air velocity produces a 2.5°C temperature drop. When the difference in porosity between meshes is not so marked, as in this study, the wind velocity is more influential. However, when the ventilation of the greenhouse is due to the thermal effect, on days with little wind, higher porosity of the insect-proof screen proves essential.

Table 6. Microclimate conditions inside greenhouses for the different tests (average values ± standard deviation): T_i, inside temperature [°C]; T_{WS} and T_{LS}, air temperature [°C] near windward and leeward vents, respectively (measured with 3D sonic anemometers and corrected with Equation [1]). ΔT_{io}, inside to outside temperature difference [°C]; η_T ventilation efficiency for the temperature. N, experimental measurement number

N	T_i	ΔT_{io}	T_{WS}	T_{LS}	η_T	T_i	ΔT_{io}	T_{WS}	T_{LS}	η_T
	Eastern sector (10 × 20 threads cm^{-2})					**Western sector (13 × 30 threads cm^{-2})**				
1	26.0 ± 0.9*	9.0	21.2 ± 0.7	22.4 ± 0.3	0.54	25.7 ± 1.0*	8.8	21.4 ± 0.9	22.8 ± 0.6	0.59
2	28.6 ± 0.5*	6.5	24.2 ± 0.9	25.8 ± 0.1	0.45	28.3 ± 0.1*	6.2	24.9 ± 0.8	26.3 ± 0.5	0.56
3	28.2 ± 0.4*	2.7	26.4 ± 1.0	27.6 ± 0.1	0.58	27.2 ± 0.5*	1.8	27.5 ± 0.7	28.0 ± 0.6	1.30
4	28.6 ± 0.2*	4.7	26.5 ± 0.6	28.2 ± 0.0	0.72	28.2 ± 0.2*	4.3	27.4 ± 0.5	28.2 ± 0.3	0.89
5	31.3 ± 0.2*	4.3	29.1 ± 0.6	30.4 ± 0.5	0.65	30.8 ± 0.4*	3.8	30.5 ± 0.7	31.0 ± 0.3	0.99
6	32.7 ± 0.5*	4.8	30.3 ± 0.6	31.5 ± 0.1	0.62	32.1 ± 0.5*	4.2	31.5 ± 1.2	32.6 ± 0.7	0.98

* Indicate statistically significant differences between eastern and western sectors (95% confidence level).

The results obtained indicate that reducing the porosity of the insect-proof screen also reduces the air exchange rate. Consequently, the porosity can also exert a considerable influence on the greenhouse inside temperature (increasing it by 0.1°C per percentage difference in mesh porosity). This negative effect on the greenhouse microclimate is particularly notable around midday when the vents are fully open. Nevertheless, during the rest of the day the negative effect can be offset by opening the windows wider. In previous works analyzing four crop cycles (2007-09) in the same greenhouse, the experimental mesh was not found to cause significant variations in mean temperature or yield (Molina-Aiz *et al*., 2012), but it did reduce the incidence of whitefly (Escamirosa, 2009).

As final conclusions, by using finer threads, insect-proof screens can be designed to combine smaller pore size and greater porosity; this results in improvements in the greenhouse microclimate due to the improved natural ventilation, which is a key feature of Mediterranean greenhouses.

In comparison to the commercial control mesh (10×20 threads cm^{-2}; 33.5% porosity), the experimental mesh (13×30 threads cm^{-2}; 39.0% porosity):

— (i) provides an 11% higher discharge coefficient at the vents ($C_{d\text{-}10 \times 20}/C_{d\text{-}13 \times 30} = 0.89$), which leads to a theoretical 11% increase in the greenhouse's natural ventilation capacity.

— (ii) does not have a negative effect on the greenhouse airflow pattern.

— (iii) produces a mean increase of 16% in the air exchange rate.

— (iv) produces a 0.5°C drop in inside temperature (0.1°C per 1% difference in porosity).

— (v) improves the ventilation efficiency for the temperature η_T (mean value of 0.9 as compared to 0.6 with the commercial mesh).

Insect-proof screens with smaller thread diameter enable a greater mesh porosity, which improves greenhouse ventilation when greater cooling is required (around midday). At the same time the pore size is reduced, which prevents the entrance of pests and the exit of beneficial insects used in Integrated Pest Management, a widespread practice in Almería's greenhouses.

Acknowledgements

This work has been financed by the *Junta de Andalucía* and the Spanish *Ministerio de Ciencia e Innovación* by means of the research grants P09-AGR-4593 and AGL2010-22284-C03-01, respectively.

References

Alvarez AJ, 2010. Analysis of the geometric characteristics and aerodynamic behaviour of insect-proof screens used in greenhouses to protect crops. Doctoral thesis. Universidad de Almería, Almería, Spain. [In Spanish].

Alvarez AJ, Oliva RM, Valera DL, 2012. Software for the geometric characterisation of insect-proof screens. Comput Electron Agric 82: 134-144.

Ansari MA, Shah FA, Whittaker M, Prasad M, Butt TM, 2007. Control of western flower thrips (*Frankliniella occidentalis*) pupae with *Metarhizium anisopliae* in peat and peat alternative growing media. Biol Control 40: 293-297.

Arbel A, Shklyar A, Barak M, 2000. Buoyancy-driven ventilation in a greenhouse cooled by a fogging system. Acta Hort 534: 327-334.

Arthurs S, Heinz KM, Thompson S, Krauter PC, 2003. Effect of temperature on infection, development and reproduction of the parasitic nematode *Thripinema nicklewoodi* in *Frankliniella occidentalis*. BioControl 48: 417-429.

ASABE Standards, 2008. EP406.4: Heating, ventilating and cooling greenhouses. ASAE, St. Joseph, MI, USA.

Baeza EJ, Pérez-Parra JJ, Montero JI, Bailey BJ, López JC, Gázquez JC, 2009. Analysis of the role of sidewall vents on buoyancy-driven natural ventilation in parral-type greenhouses with and without insect screens using computational fluid dynamics. Biosyst Eng 104: 86-96.

Bailey BJ, 2003. Screens stop insects but slow airflow. Fruit Veg Tech 3: 6-8.

Bailey BJ, Montero JI, Pérez-Parra JJ, Robertson AP, Baeza E, Kamaruddin R, 2003. Airflow resistance of greenhouse ventilators with and without insect screens. Biosyst Eng 86(2): 217-229.

Baker JR, Jones RK, 1989. Screening as part of insect and disease management in the greenhouse. North Carolina Flower Growers' Bulletin 34: 1-9.

Bartzanas T, Boulard T, Kittas C, 2002. Numerical simulation of the airflow and temperature distribution in a tunnel greenhouse equipped with insect-proof screen in the openings. Comput Electron Agric 34: 207-221.

Berlinger MJ, Leblush-Mordechl S, Fridja D, Mor N, 1992. The effect of types of greenhouse screens on the presence of western flower thrips: a preliminary study. OILB-SROP Bull 16(2): 13-19.

Boulard T, Meneses JF, Mermier M, Papadakis G, 1996. The mechanisms involved in the natural ventilation of greenhouses. Agric Forest Meteorol 79: 61-77.

Boulard T, Feuilloley P, Kittas C, 1997. Natural ventilation performance of six greenhouse and tunnel types. J Agr Eng Res 67(4): 249-266.

Boulard T, Kittas C, Papadakis G, Mermier M, 1998. Pressure field and airflow at the opening of a naturally ventilated greenhouse. J Agr Eng Res 71: 93-102.

Boulard T, Wang S, Haxaire R, 2000. Mean and turbulent air flows and microclimatic patterns in an empty greenhouse tunnel. Agric Forest Meteorol 100: 169-181.

Campen JB, 2005. Greenhouse design applying CFD for Indonesian conditions. Acta Hort 691: 419-424.

Campen JB, Bot GPA, 2003. Determination of greenhouse specific aspects of ventilation using three dimensional computational fluid dynamics. Biosyst Eng 84(1): 69-77.

Castañé C, Alomar O, Goula M, Gabarra R, 2004. Colonization of tomato greenhouses by the predatory mirid bugs *Macrolophus caliginosus* and *Dicyphus tamaninii*. Biol Control 30: 591-597.

Dierickx IE, 1998. Flow reduction of synthetic screens obtanined with both a water and airflow apparatus. J Agr Eng Res 71: 67-73.

Escamirosa C, 2009. Analysis of the effect of new anti-insect methods on several crops in Mediterranean greenhouses. Doctoral thesis. Universidad de Almería, Almería, Spain. [In Spanish].

Fatnassi H, Boulard T, Demrati H, Bouirden L, Sappe G, 2002. Ventilation performance of a large Canarian-type greenhouse equipped with insect-proof nets. Biosyst Eng 82(1): 97-105.

Fatnassi H, Boulard T, Bouirden L, 2003. Simulation of climatic conditions in full-scale greenhouse fitted with insect-proof screens. Agric Forest Meteorol 118: 97-111.

Fatnassi H, Boulard T, Poncet C, Chave M, 2006. Optimisation of greenhouse insect screening with computational fluid dynamics. Biosyst Eng 93(3): 301-312.

Forchheimer P, 1901. Easserbewegung durch boden. Z Ver Deutsch 45: 1782-1788.

Harmanto, Tantau H, Salokhe VM, 2006. Microclimate and air exchange rates in greenhouses covered with different nets in the humid tropics. Biosyst Eng 94(2): 239-253.

Hellickson MA, Walker JN, 1983. Ventilation of agricultural structures. ASAE Monograph No 6. ASABE, St Joseph, MI, USA.

Hilje L, Stansly PA, 2008. Living ground covers for management of *Bemisia tabaci* (Gennadius) (Homoptera: Aleyrodidae) and tomato yellow mottle virus (ToYMoV) in Costa Rica. Crop Prot 27: 10-16.

Hoddle MS, van Driesche RG, Elkinton JS, Sanderson JP, 1998. Discovery and utilization of *Bemisia argentifolii* patches by *Eretmocerus eremicus* and *Encarsia formosa* (Beltsville strain) in greenhouses. Entomol Exp Appl 87: 15-28.

Katsoulas N, Bartzanas T, Boulard T, Mermier M, Kittas C, 2006. Effect of vent openings and insect screens on greenhouse ventilation. Biosyst Eng 93(4): 427-436.

Kittas C, Boulard T, Papadakis G, 1997. Natural ventilation of a greenhouse with ridge and side openings: sensitivity to temperature and wind effects. T ASAE 40(2): 415-425.

Kittas C, Boulard T, Bartzanas T, Katsoulas N, Mermier M, 2002. Influence of an insect screen on greenhouse ventilation. T ASAE 45(4): 1083-1090.

Kittas C, Katsoulas N, Bartzanas T, Mermier M, Boulard T, 2008. The impact of insect screens and ventilation openings on the greenhouse microclimate. T ASABE 51(6): 2151-2165.

Kosmos SR, Riskowski GL, Christianson LL, 1993. Force and static pressure resulting from airflow through screens. T ASAE 36(5): 1467-1472.

Linker R, Tarnopolsky M, Seginer I, 2002. Increased resistance to flow and temperature-rise resulting from dust accumulation on greenhouse insect-proof screens. ASAE Ann Int Meeting, Chicago (USA), July 28-31. Paper 024040.

López A, Valera DL, Molina-Aiz FD, 2011. Sonic anemometry to measure natural ventilation in greenhouses. Sensors 11: 9820-9838.

López A, Valera DL, Molina-Aiz FD, Peña A, 2012. Sonic anemometry measurements to determine airflow patterns in multi-tunnel greenhouse. Span J Agric Res 10(3): 631-642.

López-Martínez A, Valera DL, Molina-Aiz FD, Peña A, Marín P, 2013. Field analysis of the deterioration after some years of use of four insect-proof screens utilized in Mediterranean greenhouses. Span J Agric Res 11(4): 958-967.

Lucas E, Alomar A, 2002. Impact of the presence of *Dicyphus tamaninii* Wagner (Heteroptera: Miridae) on whitefly (Homoptera: Aleyrodidae) predation by *Macrolophus caliginosus* (Wagner) (Heteroptera: Miridae). Biol Control 25: 123-128.

Mainali BP, Lim UT, 2008. Use of flower model trap to reduce the infestation of greenhouse whitefly on tomato. J Asia Pac Entomol 11: 65-68.

Miguel AF, Van de Braak NJ, Bot GPA, 1997. Analysis of the airflow characteristics of greenhouse screening materials. J Agr Eng Res 67: 105-112.

Molina-Aiz FD, 2010. Ventilation simulation and modelling by computational fluid dynamics (CFD) in Almería-type greenhouses. Doctoral thesis. Universidad de Almería, Almería, Spain. [In Spanish].

Molina-Aiz FD, Valera DL, Álvarez AJ, 2004. Measurement and simulation of climate inside Almería-type greenhouses using computational fluid dynamics. Agric Forest Meteorol 125: 33-51.

Molina-Aiz FD, Valera DL, Álvarez AJ, Madueño A, 2006. A wind tunnel study of airflow through horticultural crops: determination of the drag coefficient. Biosyst Eng 93(4): 447-457.

Molina-Aiz FD, Valera DL, Peña AA, Gil JA, López A, 2009. A study of natural ventilation in an Almería-type greenhouse with insect screens by means of tri-sonic anemometry. Biosyst Eng 104: 224-242.

Molina-Aiz FD, Valera DL, López A, Álvarez AJ, Escamirosa C, 2012. Effects of insect-proof screens used in greenhouse on microclimate and fruit yield of tomato (*Solanum lycopersicum* L.) in a mediterranean climate. Acta Hort 927: 707-714.

Montero JI, Muñoz P, Anton A, 1997. Discharge coefficients of greenhouse windows with insect-proof screens. Acta Hort 443: 71-77.

Muñoz P, Montero JI, Antón A, Giuffrida F, 1999. Effect of insect-proof screens and roof openings on greenhouse ventilation. J Agr Eng Res 73: 171-178.

Nield DA, Bejan A, 1998. Convection in porous media. Springer, NY (USA).

Papadakis G, Mermier M, Meneses JF, Boulard T, 1996. Measurement and analysis of air exchange rates in a greenhouse with continuous roof and side openings. J Agr Eng Res 63: 219-228.

Pérez-Parra JJ, Baeza E, Montero JI, Bailey BJ, 2004. Natural ventilation of parral greenhouses. Biosyst Eng 87: 89-100.

Qingyan C, Van der Kooi J, Meyers AT, 1988. Measurements and computations of ventilation efficiency and temperature efficiency in a ventilated room. Energ Buildings 12(2): 85-99.

Shilo E, Teitel M, Mahrer Y, Boulard T, 2004. Air-flow patterns and heat fluxes in roof-ventilated multi-span greenhouse with insect-proof screens. Agric Forest Meteorol 122: 3-20.

Shipp JL, Wang K, 2003. Evaluation of *Amblyseius cucumeris* (Acari: Phytoseiidae) and *Orius insidiosus* (Hemiptera: Anthocoridae) for control of *Frankliniella occidentalis* (Thysanoptera: Thripidae) on greenhouse tomatoes. Biol Control 28: 271-281.

Tanaka N, Matsuda Y, Kato E, Kokabe K, Furukawa T, Nonomura T, Honda K, Kusakari S, Imura T, Kimbara J, Toyoda H, 2008. An electric dipolar screen with oppositely polarized insulators for excluding whiteflies from greenhouses. Crop Prot 27: 215-221.

Tanny J, Haslavsky V, Teitel M, 2008. Airflow and heat flux through the vertical opening of buoyancy-induced naturally ventilated enclosures. Energ Buildings 40: 637-646.

Taylor RAJ, Shalhevet S, Spharim I, Berlinger MJ, Lebiush-Mordechi S, 2001. Economic evaluation of insect-proof screens for preventing tomato yellow leaf curl virus of tomatoes in Israel. Crop Prot 20: 561-569.

Teitel M, 2001. The effect of insect-proof screens in roof openings on greenhouse microclimate. Agric Forest Meteorol 110(1): 13-25.

Teitel M, 2007. The effect of screened openings on greenhouse microclimate. Agric Forest Meteorol 143(3-4): 159-175.

Teitel M, Shklyar A, 1998. Pressure drop across insect-proof screens. T ASAE 41(6): 1829-1834.

Teitel T, Tanny J, Ben-Yakir D, Barak M, 2005. Airflow patterns through roof openings of a naturally ventilated greenhouse and their effect on insect penetration. Biosyst Eng 92(3): 341-353.

Teitel M, Liran O, Tanny J, Barak M, 2008. Wind driven ventilation of a mono-span greenhouse with a rose crop and continuous screened side vents and its effect on flow patterns and microclimate. Biosyst Eng 101(1): 111-122.

Valera DL, Álvarez AJ, Molina FD, Peña A, López JA, Madueño A, 2003. Caracterización geométrica de diferentes tipos de agrotextiles utilizados en invernaderos. Proc II Congreso Nacional de Agroingeniería, Córdoba (Spain), Sept 24-16. pp: 670-675.

Valera DL, Molina FD, Álvarez AJ, López JA, Terrés-Nicoli JM, Madueño A, 2005. Contribution to characterization of insect-proof screens: experimental measurements in wind tunnel and CFD simulation. Acta Hort 691: 441-448.

Valera DL, Álvarez AJ, Molina FD, 2006. Aerodynamic analysis of several insect-proof screens used in greenhouses. Span J Agric Res 4(4): 273-279.

Van Buggenhout S, Van Brecht A, Eren Özcan S, Vranken E, Van Malcot W, Berckmans D, 2009. Influence of sampling positions on accuracy of tracer gas measurements in ventilated spaces. Biosyst Eng 104: 216-223.